Efficient Beamforming Training for 60-GHz Millimeter-Wave Communications: A Novel Numerical Optimization Framework

Bin Li, Zheng Zhou, *Member, IEEE*, Haijun Zhang, and Arumugam Nallanathan, *Senior Member, IEEE*

***Abstract*—In this paper, we formulate realistic beamforming (BF) training (or beam steering) in the emerging 60-GHz millimeter-wave communications as a numerical optimization problem. To maximize the receiving SNR, it aims to identify the optimal beam pair from a prescribed codebook using as little overhead as possible. Being a promising numerical method that excludes a functional derivative, the Rosenbrock numerical search may be of great significance to such applications. Nevertheless, for the encountered nonsmooth objective function, a search failure is inevitable due to the local optimum. To meet this challenge, we further present an appealing global numerical algorithm inspired by simulated annealing (SA) mechanics. In sharp contrast to classical schemes, numerical probes that lead to reward improvement are always accepted, and search moves toward worse solutions are also permitted, with a probability associated with an external temperature parameter. By relying on a newly designed two-level annealing schedule, the temperature decreases; thereby, permitting movements to worse solutions is progressively restricted. Consequently, it can basically escape from the local optimum. We then apply this new numerical search to beam switching of 60-GHz communications. Experimental simulations have demonstrated that the developed beam-switching scheme can efficiently discover the optimal beam pair by considerably reducing protocol overhead and energy consumption.**

***Index Terms*—Beam training, energy efficient, Rosenbrock search, simulated annealing (SA), two-level annealing, 60-GHz millimeter-wave communications.**

I. Introduction

As a promising way to enhance spectral efficiency via directional transmission, beamforming (BF) has been widely adopted in currently emerging wireless communications [1]. In the 60-GHz millimeter-wave wireless personal area networks (WPANs) and wireless local area networks (WLANs), multiple-antenna-based BF is also recommended to compensate the noticeable path loss and to allow space-division multiple access [2]–[4]. Considering the popular suboptimal analogy BF with a group of predefined beam patterns (i.e., a codebook) [5], [6], in the BF training stage (or beam switching), the transceiver and the receiver will determine the best beam pattern for subsequent data streams. This procedure is generally a bidirectional sequence of BF training frame transmissions (i.e., protocol overhead), providing necessary signaling between two involved devices [7].

It is apparent that, for realistic high-speed applications, fast beam switching is not only significant to reduce protocol overhead (i.e., the number of preambles) but is also meaningful to minimize power consumption and to thereby improve the energy efficiency of 60-GHz communications [7]. Unfortunately, relying on an exhaustive search, the existing popular two-stage scheme requires remarkable protocol overhead [2], [6], [7]. Thus, by consuming considerable device energy, it is inefficient and infeasible to find the optimal beam patterns within the current processing framework.

To develop efficient BF training for 60-GHz communications, from an appealing numerical optimization point of view, in this paper, we formulate the beam-switching process as a finite-space search problem. Within the 2-D search space consisting of two pattern indexes from the prescribed beam codebook, it tries to identify the optimal transmitter–receiver (Tx–Rx) beam pair maximizing the receiving SNR using as less protocol overhead (and energy) as possible. When the derivatives of the reward function (i.e., the receiving SNR) are practically available, the conjugate gradient may be utilized to effectively solve this problem [8]. Unfortunately, the objective function in beam switching can be only evaluated after one beam pair has been used for transmission [5], [6]. That is, the operating reward function here can be only determined in time by experimental trials, not to mention its analytic derivative as *a priori*.

This situation has greatly promoted the need for an efficient numerical search method that can essentially exclude the function gradient information. The Rosenbrock search is much applicable to the optimization problem in which the explicit derivative cannot be efficiently computed, yet the objective function is inexpensive to calculate [9]–[11]. In this direct numerical scheme, instead of calculating the steepest gradient, only simple evaluations on the reward function are

Manuscript received August 6, 2012; revised December 14, 2012 and May 16, 2013; accepted July 10, 2013. Date of publication August 26, 2013; date of current version February 12, 2014. This work was supported in part by the National Natural Science Foundation of China under Grant 60772021, Grant 60972079, and Grant 60902046, by the Important National Science and Technology Specific Projects under Grant 2009ZX03006-006/-009, and by the Korean Ministry of Knowledge Economy through the Information Technology Research Center Support Program supervised by the National IT Industry Promotion Agency under Grant NIPA-2011-C1090-1111-0007. The review of this paper was coordinated by Dr. H. Lan.

B. Li, Z. Zhou, and H. Zhang are with the School of Information and Communication Engineering, Beijing University of Posts and Telecommunications, Beijing 100876, China (e-mail: stonebupt@gmail.com).

A. Nallanathan is with the Institute of Telecommunications, King's College London, London WC2R 2LS, U.K.

Color versions of one or more of the figures in this paper are available online at http://ieeexplore.ieee.org.

Digital Object Identifier 10.1109/TVT.2013.2279694

required. By implicitly approaching the function gradient through a two-step search (i.e., probes and pattern moves) [10], this numerical mechanics usually exhibits a promising search ability.

Nevertheless, when encountering nonsmooth objective functions containing numerous local optimum values, the Rosenbrock numerical method may be easily driven into local regions, leading to search failures [12]. Unfortunately, the receiving SNRs may exhibit numerous local maxima, as will be shown later. Thereby, despite the merit of excluding functional derivatives, the Rosenbrock method cannot be directly applied to realistic BF training, given the high probability of search failures. As highlighted, this difficulty is also common to other numerical techniques, such as the simplex method [13] and the Powell search [14]. These numerical methods are in essence premised on a greedy conception [15], i.e., only search moves resulting in better reward could be accepted. As a consequence, it is natural that these hill-climbing algorithms may inevitably fall into the local optimum.

In this paper, we first develop an efficient global numerical algorithm by emulating the physical annealing process [16], [17] and then apply it to solve the beam-switching problem from an appealing numerical optimization perspective. The new scheme may dramatically alleviate the overhead burden. Thus, the energy consumption of the 60-GHz BF training process can be reduced. Correspondingly, the main contributions of this paper are twofold.

A. SA-Inspired Numerical Search

To overcome the aforementioned defect of classical numerical techniques, we introduce simulated annealing (SA) mechanics to the Rosenbrock method, and we further design a promising numerical optimization algorithm. Being analogous to the physical annealing process [16], [18], during the new numerical search excluding the analytic objective function, the search probes toward worse reward are also accepted with a probability rather than only permitting the search moves to better solutions [19]. This acceptance probability is determined by a time-varying temperature parameter [20]. As the search proceeds, the external temperature is gradually reduced, accompanying the probability of allowing worse moves, and subsequent search will focus on the potential region [21]. Finally, our new scheme degrades to a direct numerical search.

It is worth noting that, nevertheless, a simple accommodation of SA to the Rosenbrock method could not guarantee a complete search success, i.e., search failures are still inevitable. In addition, the required search steps may be unaffordable. To remedy these problems, by constructively integrating with the two-step mechanics, i.e., probe and pattern moves, a novel two-level temperature control scheme is designed, which serves as a special kind of neighbor exploitation and can significantly enhance search performance. The developed SA-inspired numerical scheme may be the global optimum values of nonsmooth functions if the presented temperature decrement (two annealing parameters) is properly configured, which provides a great promise to various realistic problems.

B. Efficient Beam Switching

By formulating 60-GHz BF training as a numerical optimization problem on a 2-D plane composed of two beam indexes, we further present an efficient beam-switching scheme based on the designed numerical algorithm. Although the analytical derivative of the reward function (e.g., the receiving SNR) is practically unavailable, this new numerical scheme can implicitly exploit the local gradient information of the objective function, leading to constructive search moves. Meanwhile, owing to the integrated SA mechanics and the resulting enhanced search ability, our proposed algorithm can ignore the local optimum involved in the nonsmooth reward function, and a complete search success can be achieved. In sharp contrast to the existing popular techniques premised on an exhaustive search, this algorithm essentially relies on *active-search* mechanics, in which each search movement could contribute to the final optimal solution. In other words, only a small portion of beam pairs will be tested using the new numerical search, whereas most of the other beam pairs will never be probed. Consequently, the suggested scheme promises to be capable of noticeable efficiency; hence, search complexity can be remarkably reduced, accompanying transmission overhead and energy consumption. Simulation results demonstrate the advantages of the suggested beam-switching algorithm over the other existing schemes, such as the state-of-the-art schemes specified by 60-GHz WPAN standardizations.

The remainder of this paper is outlined as follows. Section II will give a full BF model and system configuration, i.e., the adopted antenna array and the popular beam-pattern codebook. Beam switching is also formulated in Section II, accompanying the existing BF training scheme approved by the current undergoing 60-GHz standardizations. Subsequently, the Rosenbrock-numerical-search-based beam-switching scheme is developed in Section III. In Section IV, a new efficient numerical search is further presented, which is then applied to realistic beam switching. Numerical simulation and performance evaluation are presented in Section V. Finally, we conclude this paper in Section VI.

II. Beam Switching in 60-GHz Wireless Personal Area Networks

Attributed to a massive amount of unlicensed spectra available at the 60-GHz band with a worldwide overlap [22]–[24], the bandwidth-demanding WPANs (and WLANs) working in such frequency bands have been gradually coming into the picture [2], [6], [7] with a promise of high-speed transmission over the relatively short range (i.e., 1–15 m). BF, which can be conveniently implemented on a small area of tiny portable devices, is widely adopted in 60-GHz millimeter-wave communications to provide significant processing gain, which may effectively compensate the tremendous path loss in this band and hence improve the link budget [2], [25].

A. System Configurations

A practical BF system model is shown in Fig. 1. Device 1 (DEV1) has N_t transmit antennas, whereas Device 2 (DEV2)

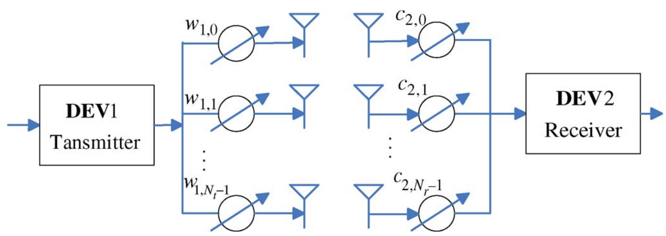

Fig. 1. System model for 60-GHz BF. Notice that, for the front-end BF, the phase shifter in radio frequency is used.

employs N_r receiver antennas. At the transmitter, the phase of the upconverted RF data stream is rotated by transmit weight vector $\mathbf{w}$ [3], [5] and is then emitted into wireless channels. Accordingly, the received signals are first weighted by reception weight vector $\mathbf{w}'$, are then combined together, and finally downconverted for baseband processing. Notice that, in practice, it usually meets $\mathbf{w} \neq \mathbf{w}'$.

Given the high power consumption of RF electrical elements and the complicated realizations, the beam-steering vector with both phase shift and amplitude adjustment seems to be impractical for 60-GHz compliant devices [2], [3], [26]. Hence, a feasible alternative with rapid processing speed is to use a phased antenna array with fixed amplitude [2]. As reported in [5], the beam codebook can be defined by $N \times K$ matrix $\mathbf{W}(N,\ K)$, which is specified by the element number N and the desired number of beams K. Each column of $\mathbf{W}$ corresponds to the phase rotations of antenna elements, generating a specific beam pattern. For 60-GHz WPANs, the $(N,\ K)$th elements of $\mathbf{W}(N,\ K)$ is given by

$$w_{n,\ k}^{(N,\ K)} = j^{f_{n,\ k}} \tag{1}$$

where

$$f_{n,\ k} = \text{floor}\left(\frac{n \times \text{mod}(k + K/4,\ K)}{K/4}\right). \tag{2}$$

In (2), $\text{floor}(x)$ denotes the biggest integer that is smaller than or equal to x, and $\text{mod}(x,\ y)$ refers to the modular operation on x with respect to y. For simplicity, we employ the 1-D uniformly spaced antenna array in the following analysis. Given the pattern codebook $\mathbf{W}$, the array factor corresponding to the kth beam-steering vector can be written as

$$A_{k,\ \theta}(\theta') = \sum_{n=0}^{N-1} w_{n,\ k} e^{j2\pi n(d/\lambda)\ \cos\ (\theta - \theta')} \tag{3}$$

where d denotes the spacing distance between two adjacent elements, and λ is the wavelength [5], [27]. The normal direction of the antenna array with respect to the x-axis is denoted by θ, which is related with the random gesture of array and remains perpendicular to the orientation of linear array elements, with the codebook index of k. θ' accounts for the signal arrival direction with respect to the x-axis. In practice, the number of beam patterns (i.e., K) and antenna elements (i.e., N) is supposed to fulfill the relationship $K = 2N$ [5], [6].

B. Beam Switching

In the context of short-range indoor communications, the intensive multipath trajectories can be observed in typical propagation of 60-GHz WPANs [28], [29]. The multipath channel model of 60 GHz is based on the well-known Saleh–Valenzuela modeling, which is specified by the IEEE 802.15.3c Task Group (TG). The unified channel impulse response (CIR) is given by [29]

$$\begin{aligned} h(t,\ \theta,\ \phi) &= \alpha_{0,\ 0}\delta(\theta - \theta_{0,\ 0})\delta(\phi - \phi_{0,\ 0})\delta(t - \tau_{0,\ 0}) \\ &\quad + \sum_{l=1}^{L}\sum_{k=1}^{K_l} \alpha_{k,\ l}\delta(\theta - \theta_{k,\ l})\delta(\phi - \phi_{k,\ l})\delta(t - \tau_{k,\ l}) \end{aligned} \tag{4}$$

where L is the number of paths (or clusters); K_l is the number of subpaths of the lth cluster; $\alpha_{k,\ l} = |\alpha_{k,\ l}| \exp(j\phi_{k,\ l})$ corresponds to the complex channel gain of the kth subpath of the lth cluster, with i.i.d. random phase $\phi_{k,\ l}$ distributed over $U[0, 2\pi)$; $\tau_{k,\ l}$ is the time delay; and $\theta_{k,\ l}$ and $\phi_{k,\ l}$ are the angle of arrival (AoA) and the angle of departure, respectively [29].

It is obvious that the integration of both time (i.e., time of arrival) and angle (i.e., AoA) produces the total received signal power. Accordingly, the SNR in the receiver can be expressed as

$$\text{SNR} = \frac{1}{\sigma_n^2}\left|\int_{\theta'}\int_{t} h(t,\ \theta',\ \varphi')A_{p,\ \theta}(\theta')A_{q,\ \phi}(\phi')dtd\theta'\right|^2 \tag{5}$$

where $A_{p,\ \theta}(\theta')$ denotes the array factor of the reception beam with the index of p, and θ is the corresponding polar angle with respect to the x-axis. σ_n^2 represents the power of additive white Gaussian noise, which is assumed to be independent of the used beam pair. Taking the discrete CIR into accounts, the receiving SNR can be written as

$$\text{SNR}(p,\ q) = \frac{1}{\sigma_n^2} \times \left|\sum_{l=1}^{L}\sum_{k=0}^{K_l} \alpha_{k,\ l}A_{p,\ \theta}(\theta_{k,\ l})A_{q,\ \phi}(\phi_{k,\ l})\right|^2. \tag{6}$$

It is worth highlighting that the summation of the different CIR weighted paths in the given objective function, with both constructive and destructive interference, may introduce frequency selectivity. In this paper, we mainly focus on a realistic situation with a complicated objective function, as in (6), i.e., by taking both the multipath propagation and frequency selectivity.

Traditionally, with the term "optimal beamforming," beam-steering vector $\mathbf{w}$ (and $\mathbf{w}'$) should be dynamically adjusted according to the provided CSI. However, such *a priori* information usually requires a dedicated feedback channel, which greatly excites the codebook-based BF. Accordingly, given the well-designed beam-steering vectors $\mathbf{W}$, BF aims to select the best beam pair $(p_{\text{opt}},\ q_{\text{opt}})$ from the predefined codebook, to maximize the receiving SNR defined by (6), i.e.,

$$(p_{\text{opt}},\ q_{\text{opt}}) = \max_{(p,\ q)} \text{SNR}(p,\ q), \qquad (p,\ q) \in \mathbb{R}^2.$$

A direct approach that is considered the most common, although not always the simplest, is the exhaustive search in which the beam-switching process employs $K_t \times K_r$ preamble transmissions. Through *round-trip* information exchanging, the two devices involved may eventually identify the best Tx–Rx beam pair $(p_{\mathrm{opt}},\ q_{\mathrm{opt}})$ [6]. Nevertheless, the resulting enormous protocol overhead may consume considerable power, which may also significantly reduce transmission efficiency. Notice that the *single-agent* essence of this problem (i.e., each reward value can be only derived from one single experiment) basically excludes the other popular biological optimization techniques, such as genetic algorithm (GA) and particle swarm optimization (PSO), which should rely on multiagents for conducting their search.

C. Previous Work

Targeting the reduced protocol overhead and energy consumption, a two-stage beam-switching scheme has recently been adopted by the 60-GHz standardizations, i.e., IEEE 802.15.3c [6], [7], which can be substantially divided into the sector-level search (SLS) and the normal beam search.

In the first stage (i.e., SLS) of the 3c scheme, sector beams are used, which are implemented by activating a small part of antenna elements, e.g., two out of 16. The best sector beam index can be found in this stage. After notifying the best sector, the transceiver and the receiver will then perform a beam search by examining the subset beams specified by the sector index in a traversal fashion [6], [30]. Let $N_t^{(1)} = N_t^{(\mathrm{sector})}$ and $N_r^{(1)} = N_r^{(\mathrm{sector})}$ be the number of sector beams (i.e., sector-level codebook size) of the transceiver and the receiver, respectively, and let $N_t^{(\mathrm{beam})} = 2N_t$ and $N_r^{(\mathrm{beam})} = 2N_r$ be the number of the normal beams (i.e., beam-level codebook size) of the transceiver and the receiver, respectively. Usually, the number of normal beams corresponding to one sector can be determined by $N_t^{(2)} = N_t^{(\mathrm{beam})}/N_t^{(\mathrm{sector})}$ and $N_r^{(2)} = N_r^{(\mathrm{beam})}/N_r^{(\mathrm{sector})}$. Thus, the total number of preamble transmissions, with which the search complexity of the two-step scheme can be conveniently measured, is given by

$$\begin{aligned} N_{3c} &= N_t^{(1)} \times N_r^{(1)} + N_t^{(2)} \times N_r^{(2)} \\ &= N_t^{(1)} \times N_r^{(1)} \left[1 + 4N_t N_r / \left(N_t^{(1)} \times N_r^{(1)}\right)^2\right]. \end{aligned} \tag{7}$$

From (7), two observations can be made to the accumulated search steps of this beam-switching method. First, there indeed exists the optimal value of the sector number for different antenna element sizes (or codebook sizes). Hence, to achieve the most favorable performance, the medium-access-control protocol should also take this into account. Second, it is noted that, although this two-stage beam switching can reduce the number of preamble transmissions, the search complexity is still on the order of $O(N_t \times N_r) \sim O(N^2)$. In other words, with the further increase in antenna elements, the required overhead and consumed energy may become unaffordable.

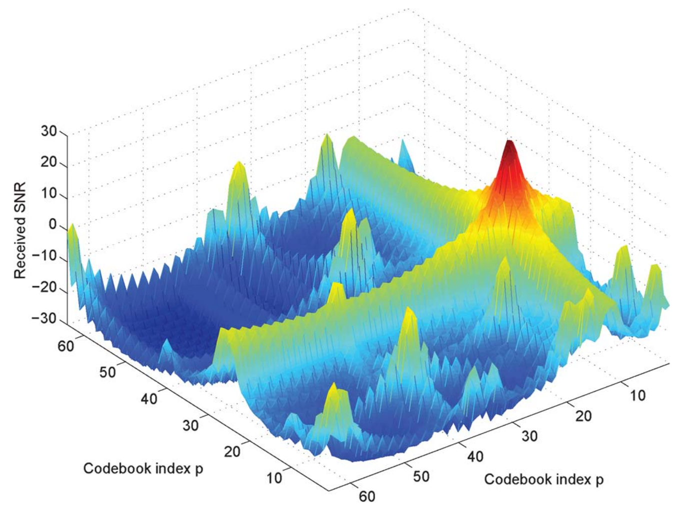

Fig. 2. Objective function of the formulated 60-GHz beam switching on 2-D beam-index plane $(p,\ q)$. Notice that the number of antenna elements is $N = 32$, and correspondingly, the total number of beams (or codebook size) is 64.

III. Rosenbrock-Method-Based Beam Switching

A. Problem Description

For the 1-D antenna array with a moderate element size, the given beam-switching scheme can indeed diminish the protocol overhead. Nevertheless, for a larger codebook size in the context of high-resolution spatial transmissions, the existing methods still require enormous preambles. Here, based on a direct Rosenbrock numerical search, we suggest a new beam-switching technique with significantly reduced overhead and energy consumption. For simplicity, we adopt the 1-D antenna array in the following elaborations.

We will treat the 60-GHz beam switching as a global optimization problem in a 2-D plane that is formed by the Tx–Rx beam pair $(p,\ q)$. The reward function is the receiving SNR, which is denoted by $f(p,\ q)$, and the objective is to identify the best beam pair maximizing this reward. The receiving SNR is shown in Fig. 2, where both the transceiver and receiver antenna elements are set to $N = 32$ (i.e., $K = 64$). It is shown in Fig. 2 that the global optimum is unimodal around the best beam pair $(p_{\mathrm{opt}},\ q_{\mathrm{opt}})$. However, there exist several local optimum values in the objective function, due to beam sidelobes and multipath propagation. Although the two-stage search is relatively much beneficial, this traversal-querying-based method is still inefficient and energy demanding [33]. Hence, a more competitive way is to search through the 2-D beam-index plane within an active numerical framework [6], [31], [32] in which each search could contribute to the final optimal solution.

B. Rosenbrock Search

By excluding the derivative of reward functions [9]–[11], the Rosenbrock direct numerical method is of particular interest to the formulated beam-switching problem, in which the analytic reward function is practically unavailable. The Rosenbrock search essentially includes two phases, i.e., probe moving and pattern moving [31], [32].

1) Probe Moving: First, probe moving along the n orthogonal directions is performed, and the new start point and the potential descent direction will be discovered. In our analysis, $n = 2$ for the 1-D antenna array.

We denoted the initial solution by $\mathbf{s}^{(1)} = [p^{(1)},\ q^{(1)}]$, the magnification factor by $\mu > 1$, and the shrinkage factor by $\nu \in (-1, 0)$. Initial directions $\mathbf{d}^{(1)}$ and $\mathbf{d}^{(2)}$ can be given by

$$\mathbf{d}^{(1)} = (1,\ 0)^T \quad \mathbf{d}^{(2)} = (0,\ 1)^T. \tag{8}$$

Notice that search directions $\mathbf{d}^{(i)} (i = 1, 2)$ are supposed to be orthonormal vectors. The initial move steps, corresponding to two search directions, are denoted by ξ_1 and ξ_2, respectively. The search start during each probe round is denoted by $\mathbf{y}^{(1)}$, and the terminated solution is denoted by $\mathbf{y}^{(n+1)}$.

Starting from the initial solution, we first probe along $\mathbf{d}^{(1)}$. If we have $f(\mathbf{y}^{(1)} + \xi_1 \mathbf{d}^{(1)}) \geq f(\mathbf{y}^{(1)})$, then this probe operation is success. Then, let

$$\mathbf{y}^{(2)} = \mathbf{y}^{(1)} + \xi_1 \mathbf{d}^{(1)} \tag{9}$$

and the probe step is updated using $\xi_1 = \mu \xi_1$, which leads to much larger moving in the next probe round. Otherwise, if $f(\mathbf{y}^{(1)} + \xi_1 \mathbf{d}^{(1)}) < f(\mathbf{y}^{(1)})$, this probe operation is failed. Then, we set

$$\mathbf{y}^{(2)} = \mathbf{y}^{(1)}. \tag{10}$$

In fact, after several probe successes, the move step will be rapidly enlarged in a geometric series. Therefore, with high probability, the probe moving in the current round may have already rashly advanced, which easily misses the optimal solution. Thus, a *backward* search, i.e., a search toward the opposite direction, is adopted in the next round. The probe step is also updated using $\xi_1 = \nu \xi_1$.

After probing along one direction $\mathbf{d}^{(1)}$, the similar probe operations will be performed on the remaining direction $\mathbf{d}^{(2)}$. Finally, the probed solution $\mathbf{y}^{(n+1)}$ can be obtained, and one probe round is finished.

Then, we begin another round of probe operation. The new start solution is set to

$$\mathbf{y}^{(1)} = \mathbf{y}^{(n+1)}. \tag{11}$$

This probe moving iteration is terminated until all the direction probes are failed. Then, after the kth iteration, the obtained new solution can be given by

$$\mathbf{s}^{(k+1)} = \mathbf{y}^{(n+1)}. \tag{12}$$

2) Pattern Moving: After the probe moving stage, a new group of orthonormal search directions will be constructed by resorting to the well-known Gram–Schmidt orthogonalization.

Following the probed results, we may have

$$\mathbf{s}^{(k+1)} = \mathbf{s}^{(k)} + \sum_{i=1}^{n} \lambda_i \mathbf{d}^{(i)} \tag{13}$$

where λ_i denotes the accumulative moving step along the ith probe direction $\mathbf{d}^{(i)}$. Further manipulations on (13) result in $\mathbf{s}^{(k+1)} - \mathbf{s}^{(k)} = \sum_{i=1,\ 2} \lambda_i \mathbf{d}^{(i)}$. It is worth observing that, from this formulation, direction $\mathbf{p} \triangleq \mathbf{s}^{(k+1)} - \mathbf{s}^{(k)}$ may give an approaching descent direction [10], [11]. During the next probe moving, the new established direction should fully consider this descent direction. Thus, the new search direction can be defined by

$$\mathbf{p}^{(j)} = \begin{cases} \mathbf{d}^{(j)}, & \lambda_j = 0 \\ \sum\limits_{i=j}^{n} \lambda_i \mathbf{d}^{(j)}, & \lambda_j \neq 0. \end{cases} \tag{14}$$

By utilizing the Gram–Schmidt orthogonalization procedure [12], the new constructed search directions can be further orthogonalized, i.e.,

$$\mathbf{q}^{(j)} = \begin{cases} \mathbf{p}^{(j)}, & j = 1 \\ \mathbf{p}^{(j)} - \sum\limits_{i=1}^{j-1} \frac{\mathbf{q}^{(i)T} \mathbf{p}^{(j)}}{\mathbf{q}^{(i)T} \mathbf{q}^{(i)}} \mathbf{q}^{(i)}, & j \geq 2. \end{cases} \tag{15}$$

A group of orthonormal directions can be derived by

$$\bar{\mathbf{d}}^{(j)} = \mathbf{q}^{(j)} / \left\| \mathbf{q}^{(j)} \right\|. \tag{16}$$

It is obvious that these constructed search directions $\bar{\mathbf{d}}^{(j)}$ are linearly independent quantities, which are also orthogonal with each other.

Then, the probe moving and direction construction will be alternately continued, until the relative change in the solution drops below a prespecified threshold η, i.e., $\|\mathbf{s}^{(k+1)} - \mathbf{s}^{(k)}\| \leq \eta$. Based on the earlier discussions, the algorithm flow of the Rosenbrock search has been summarized in *Algorithm 1*.

Algorithm 1 Rosenbrock Search

Input: The predefined codebook $(p,\ q)$, the maximum presearch iterations χ, and the parameters of the Rosenbrock search, i.e., $\{\mathbf{d}^{(1)}, \mathbf{d}^{(2)}\}$, $\{\xi_1^{(0)}, \xi_1^{(0)}\}$, μ, ν, η_1, and η_2.

Output: The searched optimal beam index $(p_{\mathrm{opt}},\ q_{\mathrm{opt}})$

1: Set the obtained beam index to be the initial solution, i.e., $\mathbf{s}^{(1)} = [p^{(i)}, q^{(i)}]$; moreover, set the initial counter $k = 1$.
2: Set the initial moving set $\{\xi_1, \xi_2\} = \{\xi_1^{(0)}, \xi_2^{(0)}\}$.
3: **for** $j = 1{-}2$ **do**
4:    **if** $f(\mathbf{y}^{(j)} + \mathrm{round}(\xi_j \mathbf{d}^{(j)})) - f(\mathbf{y}^{(j)}) > 0$ **then**
5:       $\mathbf{y}^{(j+1)} = \mathbf{y}^{(j)} + \xi_j \mathbf{d}^{(j)}$, $\xi_j = \mu \times \xi_j$.
6:    **else**
7:       $\mathbf{y}^{(j+1)} = \mathbf{y}^{(j)}$, $\xi_j = \nu \times \xi_j$.
8:    **end if**
9: **end for**
10: **if** $f(\mathbf{y}^{(n+1)}) \geq f(\mathbf{y}^{(1)})$ **then**
11:    Set $\mathbf{y}^{(1)} = \mathbf{y}^{(n+1)}$, $j = 1$, return to Step 4.
12: **else**
13:    Go to Step 15.
14: **end if**
15: **if** $f(\mathbf{y}^{(n+1)}) \geq f(\mathbf{s}^{(k)})$ **then**

16: Jump to Step 22.
17: **else if** $|\xi_j| \leq \eta_1$ **then**
18: Terminate the beam search, and output the best solution $\mathbf{s}^{(k)}$.
19: **else**
20: Set $\mathbf{y}^{(1)} = \mathbf{y}^{(n+1)}$, and jump to Step 3.
21: **end if**
22: Let $\mathbf{s}^{(k)} = \mathbf{y}^{(n+1)}$, and set $\mathbf{s}^{(k)} = \mathrm{round}(\mathbf{s}^{(k)})$.
23: **if** $|\mathbf{s}^{(k+1)} - \mathbf{s}^{(k)}| < \eta_2$ **then**
24: Terminate the beam search, and output the solution $\mathbf{s}^{(k+1)}$.
25: **else**
26: Calculate the moving steps λ_i, $(i = 1, 2)$, and construct the new probing direction $\overline{\mathbf{d}}^{(j)} (j = 1, 2)$ according to (14)–(16).
27: Set $\{\xi_1, \xi_2\} = \{\xi_1^{(0)}, \xi_2^{(0)}\}$, $\mathbf{y}^{(1)} = \mathbf{s}^{(n+1)}$, and $k++$, and return to Step 3.
28: **end if**
29: Return the identified optimal beam index $(p_{\mathrm{opt}},\ q_{\mathrm{opt}})$.

C. Rosenbrock-Search-Based Beam Switching

To apply the above Rosenbrock numerical search to 60-GHz beam switching, it is necessary to make some mechanic assumptions. First, it is assumed that only one device involved can run the search engine, which is referred to as the *initiator*. The other device only changes its beams cooperatively by following the feedback information from the initiator, which is named the *responder*. The main purpose of such mechanics is to save the device energy. Second, the feedback information from the responder can be realized with the frame structure specified by current standardizations [33]. For example, the sector sweep (SS) frame can be used to convey cooperative information between two devices [7]. The only difference is that the reservation domain is no longer required, which is replaced by the training completion acknowledge field. Before identifying the best beam pair, this field is always set to 0.

Based on the given assumptions, the generalization of the Rosenbrock search to beam switching is straightforward. Each moving step in the 2-D plane will be cooperatively implemented by the initiator and the responder. Once the solution updating is completed, the initiator will use the new beam index p and simultaneously notify the responder as the next index q. As a result, the new beam pair $(p,\ q)$ will be used in the next round of moving operation. It is noted that, during this Rosenbrock search, certain beam pairs will be tested for several times. To avoid periodically repeating the same beam, a register may be suggested to record the searched path and the corresponding function value $f(p,\ q)$ so that the initiator can calculate the new move without notifying the responder of the already tested beams. Thus, the protocol overhead, which equals roughly to the accumulated search steps, is also proportional to the length of the SS frame.

D. Practical Considerations

It is observed in Fig. 2 that the target region in the 2-D plane containing the optimal beam pair is relatively small. After many probing successes, the moving step of the Rosenbrock search may be amplified without restriction [10], [11]. Consequently, the overstripped probe moving may inevitably pass the optimal solution. In practice, one efficient remedy can be suggested to the Rosenbrock numerical search. Usually, the achieved optimal reward f can be estimated by $20 \times \log_{10}(N)$ dB, where N is the number of antenna elements. Accordingly, the probing step is not only related with the previous success search but is also determined by the improvement in the reward function. Specifically, if $f(\mathbf{y}^{(j)} + round(\xi_j \mathbf{d}^{(j)})) - f(\mathbf{y}^{(j)}) > \kappa \times 20 \log_{10}(N)$, then the moving step will be clamped to 1. Here, parameter $\kappa \in (0, 1]$ is used to reinforce search efficiency, and neither a large value nor a small value can operate well. Based on our simulation experiments, κ can be empirically set to 0.5–0.8 in practice. Moreover, it is also worth noting that the practical indexes (i.e., p and q) are integers. Therefore, the output beam pattern used in the next probe moving should be rounded to the nearest integer.

It should be emphasized that, in Fig. 2, there indeed are many local optimum values in the nonsmooth reward function. Hence, the Rosenbrock search may inevitably fall into the local optimum values and terminate the search by eventually returning a nonoptimal beam pair [10], [15]. Usually, bad initiation $(p^{(1)}, q^{(1)})$ may drive the search into local optimum, whereas only a good initialization could lead to search success. Thus, a direct numerical search is much susceptible to initialization solution and hence may be still hardly applied to realistic beam switching with remarkable search failures. This problem can be partly addressed by a presearch process exploring the structures of beam patterns, in which the number of active antenna elements will be gradually increased [33]. However, there still exist two practical difficulties. First, active element adjustment means to modify the amplitude of antennas, which may contradict the low-complexity and low-power requirements. More importantly, relying on the small-region dividing and conquering conception, this presearch may become invalid due to practical imperfections.

IV. New Numerical-Search-Based Beam Switching

A. Simulated Annealing

SA is a biological algorithm designed for finding the global minimum of a cost function that possesses several local minima [16]. As a generalization of the Monte Carlo method, SA emulates the natural physical process in which the liquids freeze or the metals recrystallize with a well-defined annealing process [17], [20]. Relying on an appealing probabilistic framework, SA can solve complex optimization problems with good quality [16]. It is logical for SA to accept all state changes leading to an energy (or cost) decrease. Nevertheless, it differs remarkably from classical methods (e.g., a greedy search) by allowing the probabilistic acceptance of worse moves (i.e., an energy increase) so that it can escape from local minima in realistic optimization.

The generalization of this Monte Carlo approach to practical optimization is straightforward [16], [17]. The current state of the thermodynamic system is analogous to the current *solution* to the problem, the energy equation for the thermodynamic system is analogous to the *objective function*, and the frozen state is analogous to the *global minimum*. Accordingly, the basic elements of the SA search in our numerical beam-switching algorithm can be elaborated as follows.

1) Cost function: For realistic application, first the cost function that gives representative state energy should be defined [18]. During the considered beam switching aiming to maximize the receiving SNR, the cost function can be described as

$$E(i) \propto \left| \sum_{l=1}^{L} \sum_{k=0}^{K_l} \alpha_{k,\,l} A_{p,\,\theta}(\theta_{k,\,l}) A_{q,\,\phi}(\phi_{k,\,l}) \right|^2. \tag{17}$$

2) Acceptance Criteria: The probability of transition from the current state $\mathbf{y}^{(i)}$ to a new candidate state $\mathbf{y}^{(i+1)}$ is specified by an acceptance probability $P(E(i), E(i+1), T)$, which depends on two energy amplitudes $E(i) = E(\mathbf{y}^{(i)})$ and $E(i+1) = E(\mathbf{y}^{(i+1)})$ and a global time-varying parameter, i.e., T [18]. Given the current temperature T, the probability of an increase in energy magnitude, i.e., $\Delta E = E(i+1) - E(i) > 0$, can be given by

$$\begin{aligned} P(\Delta E,\, T) &= \frac{\exp\left(-E(i+1)/kT\right)}{\exp\left(-E(i)/kT\right) + \exp\left(-E(i+1)/kT\right)} \\ &\simeq \exp(-\Delta E/kT) \end{aligned} \tag{18}$$

where k is referred to as Boltzmann's constant [19]. It can be usually dropped directly from (18) for analysis simplicity, without affecting search performance.

When it comes to realistic optimization, SA first calculates the new energy $E(i+1)$ of the representative problem. If the energy has decreased, i.e., $\Delta E < 0$, the state transition (or search movement) from $\mathbf{y}^{(i)}$ to $\mathbf{y}^{(i+1)}$ is accepted immediately, and the system state will be changed to the new one. Otherwise, if the energy has increased, i.e., $\Delta E > 0$, the new state $\mathbf{y}^{(i+1)}$ may be still permitted using the probability returned by (18). The probability of accepting a worse state (i.e., $E(i+1) > E(i)$) is given by $\exp(-\Delta E/T)$, and the state transition happens if the following condition is satisfied:

$$P(\Delta E,\, T) \geq \gamma \tag{19}$$

where γ is a random number between 0 and 1, i.e., $\gamma \sim U(0, 1]$. From (18) and (19), it is expected that, as the temperature T decreases, the probability of allowing energy to increase is also reduced. If temperature T approach zero (or small enough), then only the better moves are accepted [18], [19].

3) Temperature Schedule: As highlighted by the given discussions, temperature parameter T is indispensable to control the ability of hill-climbing [19]. At the beginning of the search, T is initialized by a large value approaching infinite so that SA can initially wander around a broad region of search space by ignoring small features of the energy function. After a short period of movements or probes, we may expect that a roughly lower (or higher) region has been discovered, and thereafter, the freedom to wander should be restricted accordingly.

It is worth noting that the temperature schedule is of great importance to search success. The representative system may easily become trapped into a local minimal state if either the initial temperature is too low or the cooling process is done insufficiently [21]. Hence, the way we choose the initial temperature T_0 and the temperature decrement strategy determines the search performance.

Practically, the SA search is expected to start with a relatively high T_0 to have a better chance of avoiding being prematurely trapped by a local minimum. Nevertheless, it is evident that higher T_0 may also result in a longer evolution sequence of $T(k)$ $(k = 0, 1, 2,)$ and may, hence, considerably slow down the rate of convergence. In this paper, we may choose

$$T_0 = 10 \times \sigma(C) \tag{20}$$

where $\sigma(C)$ denotes the standard deviation of the reward function evaluated at $T_0 = \infty$. As is indicated in [34], $\sigma(C)$ and the corresponding expectation $E(C)$ can be estimated by resorting to a numerical approach. Nevertheless, the numerical estimation may also inevitably consume considerable overhead and energy. Alternatively, to obtain $\sigma(C)$, we may resort to an analytic method. In practice, given the number of elements N, array factor $A_{k,\,\varphi}(\theta)$ can be further expressed as [35]

$$A_{k,\,\varphi}(\theta) = N e^{j(N-1)\beta/2} \times \frac{\sin\left(N\beta/2\right)}{N \sin(\beta/2)} \tag{21}$$

where $\beta(\varphi) = 2\pi d \sin(\theta - \varphi)/\lambda$. Hence, the cumulative array factor in the receiver can be written as

$$|A(\phi, \varphi, \theta)| = \frac{\sin\left(N\beta(\phi)/2\right)\, \sin\left(N\beta(\varphi)/2\right)}{\sin\left(\beta(\phi)/2\right)\, \sin\left(\beta(\varphi)/2\right)}. \tag{22}$$

Here, both the normal direction of the transmitter (i.e., ϕ) and the receiver (i.e., φ) range from 0 to π. Then, expectation $E(C)$ and variance $\sigma(C)$ can be approximated, respectively, by

$$E(C) = \frac{1}{\pi^2} \iiint\limits_{\phi,\varphi,\theta} |A(\phi, \varphi, \theta)|^2 \, d\phi \, d\varphi \, d\theta \tag{23}$$

$$\sigma(C) = \frac{1}{\pi^2} \iiint\limits_{\phi,\varphi,\theta} \left[|A(\phi, \varphi, \theta)|^2 - E(C) \right]^2 d\phi \, d\varphi \, d\theta. \tag{24}$$

Notice that, the attenuation factor from propagation has been assumed to be 1 in the given derivation, whereas its realistic value can be conveniently evaluated using several times of pilot transmissions.

Other than a high initial temperature, a gradual reduction of temperature is also required as the search proceeds. For the formulated objective function that involves many local optimum values, we may resort to the standard geometric cooling schedule [21]. Therefore, we have

$$T(k) = T_0 \times \kappa^k, \qquad 0 < \kappa < 1. \tag{25}$$

Here, k accounts for the updating iterator. As most empirical researches have shown, decay parameter κ can be feasibly ranged in [0.05, 0.3], with the better results being found in the lower of this range [21]. As a compromise, however, the higher the value of κ is, the slower it will take the temperature decrease to the stopping criterion.

B. New Numerical Search

By presenting a novel temperature schedule and further properly accommodating SA mechanics into the Rosenbrock method, we develop a more efficient numerical search algorithm. During this new numerical scheme, we apply the probabilistic acceptance criterion to the probe moving and then construct the new search directions.

As shown by our experiments, the simple accommodation of SA into the Rosenbrock method may still easily fall into the local optimum. Hence, rather than only employing one temperature parameter as in the classical SA algorithm [16], [18], [21], two external temperature parameters T_l and T_g are suggested in the new method, i.e., the local and global temperatures, which correspond to the inner search loop (i.e., probe moving) and the outer loop (i.e., pattern moving) of the direct numerical algorithm, respectively. For each outer iteration k_global, we will initialize $T_l = T_g$ during the inner iterations k_local and then update $T_l = T_g \times \kappa_l^{k\_\text{local}}$ after probe moving. Subsequently, for two successive outer iterations $k\_\text{global}+1$ and k_global, we will update the global temperature by $T_g(k\_\text{global}+1) = T_g(k\_\text{global}) \times \kappa_g$.

The inner iteration corresponds to the probe moving of the Rosenbrock search.

1) If we have $f(\mathbf{y}^{(1)} + \xi_1 \mathbf{d}^{(1)}) \geq f(\mathbf{y}^{(1)})$, this current probe operation is successful, and we will let $\mathbf{y}^{(2)} = \mathbf{y}^{(1)} + \xi_1 \mathbf{d}^{(1)}$. Simultaneously, the probe step is updated using $\xi_1 = \mu\xi_1$.
2) Otherwise, if $f(\mathbf{y}^{(1)} + \xi_1 \mathbf{d}^{(1)}) < f(\mathbf{y}^{(1)})$, then this probe operation is a failure. In this case, we will generate a random variable $\gamma \sim U[0,1]$.
    a) If the calculated acceptance probability, i.e., $P = \exp(\Delta E/T_l)$, is larger than γ, we still allow this move, and let $\mathbf{y}^{(2)} = \mathbf{y}^{(1)} + \xi_1 \mathbf{d}^{(1)}$. Meanwhile, ξ_1 is still updated by $\xi_1 = \nu\xi_1$.
    b) Else, if $P \leq \gamma$, the current search move will not be permitted. That is, we will let $\mathbf{y}^{(2)} = \mathbf{y}^{(1)}$, and notice that the probe step is now updated by $\xi_1 = \nu\xi_1$. After the given probabilistic acceptance, the local temperature T_l is further updated using $T_l(k\_\text{local}) = T_g \times \kappa_l^{k\_\text{local}}$, and k_local is then increased by 1.

Algorithm 2 Proposed Beam-Switching Algorithm (Part I: *Complete Algorithm Flow*)

Input: Predefined codebook $(p,\ q)$, maximum presearch iterations χ, and the parameters of the Rosenbrock search, i.e., $\{\mathbf{d}^{(1)}, \mathbf{d}^{(2)}\}$, $\{\xi_1^{(0)}, \xi_1^{(0)}\}$, μ, ν, η_1, and η_2.
Output: The searched optimal beam index $(p_{\text{opt}},\ q_{\text{opt}})$

1: Set the obtained beam index to be the initial solution $\mathbf{s}^{(1)} = [p^{(i)}, q^{(i)}]$. Then, set the initial counter $k\_\text{global} = 1$ and $\text{clamp\_flag} = 0$.
2: Set the initial moving set $\{\xi_1, \xi_2\} = \{\xi_1^{(0)}, \xi_2^{(0)}\}$, and $T_g = T_0$.
3: Perform the probe moving search, according to a probabilistic mechanic (see Part II: Subprogram).
4: **if** $f(\mathbf{y}^{(n+1)}) > f(\mathbf{y}^{(1)})$ **then**
5: **if** $f(\mathbf{y}^{(n+1)}) - f(\mathbf{y}^{(1)}) > \kappa \times 20 \log_{10} M$ **then**
6: Set $\text{clamp\_flag} = 1$.
7: **end if**
8: Set $\mathbf{y}^{(1)} = \mathbf{y}^{(n+1)}$, return to Step 3.
9: **else**
10: Go to Step 12.
11: **end if**
12: **if** $f(\mathbf{y}^{(n+1)}) > f(\mathbf{s}^{(k)})$ **then**
13: Set $\mathbf{s}^{(k)} = \mathbf{y}^{(n+1)}$, and $\mathbf{s}^{(k)} = \text{round}(\mathbf{s}^{(k)})$
14: **if** $|\mathbf{s}^{(k+1)} - \mathbf{s}^{(k)}| < \eta_2$ **then**
15: Terminate the beam search and output the solution $\mathbf{s}^{(k)}$.
16: **else**
17: Calculate the moving steps λ_i, $(i = 1, 2)$, and construct the new probing direction $\overline{\mathbf{d}}^{(j)} (j = 1, 2)$ according to (14)–(16).
18: Set $\{\xi_1, \xi_2\} = \{\xi_1^{(0)}, \xi_2^{(0)}\}$, $\mathbf{y}^{(1)} = \mathbf{s}^{(n+1)}$, and $k++$
19: $T_g = T_0 \times \kappa_g^{k\_\text{global}}$, and $k\_\text{global} = k\_\text{global} + 1$. Return to Step 3.
20: **end if**
21: **else if** $|\xi_1| \leq \eta_1$ && $|\xi_2| \leq \eta_2$ **then**
22: Terminate the beam search, and output the best solution $\mathbf{s}^{(k)}$.
23: **else**
24: Set $\mathbf{y}^{(1)} = \mathbf{y}^{(n+1)}$, and jump to Step 3.
25: **end if**
26: Return the identified optimal beam index $(p_{\text{opt}},\ q_{\text{opt}})$.

The outer iteration refers to the moving of the Rosenbrock search. Once the termination condition on inner iterations has been satisfied, i.e., the probe moves of all directions are failed [9], a group of new probe directions will be constructed according to (13)–(16). Subsequently, the outer iterator will be updated, i.e., $k\_\text{global} = k\_\text{global} + 1$, and the global temperature T_g is decreased using $T_g(k\_\text{global}) = T_0 \times \kappa_g^{k\_\text{global}}$.

Algorithm 3 Proposed Beam-Switching Algorithm (Part II: *Subprogram of Step 3 in Part I*)

1: $k_{\text{local}} = 1$, $T_l = T_g$
2: **for** $j = 1\text{–}2$ **do**
3: **if** $f(\mathbf{y}^{(j)} + \text{round}(\xi_j \mathbf{d}^{(j)})) - f(\mathbf{y}^{(j)}) > 0$ **then**
4: $\mathbf{y}^{(j+1)} = \mathbf{y}^{(j)} + \xi_j \mathbf{d}^{(j)}$
5: **if** $\text{clamp\_flag} = 0$ **then**
6: $\xi_j = \mu \times \xi_j$, $j = 1, 2$.
7: **else**
8: $\xi_j = 1$.
9: **end if**
10: **else**
11: Calculate the energy decrease $\Delta E = f(\mathbf{y}^{(j)}) - f(\mathbf{y}^{(j)} + \text{round}(\xi_j \mathbf{d}^{(j)}))$.

Obtain the acceptance probability $P = \exp(-\Delta E/T_l)$.
Generate random variable $\gamma \sim U[0, 1]$.
if $\gamma \leq P$ **then**
  $\mathbf{y}^{(j+1)} = \mathbf{y}^{(j)} + \xi_j \mathbf{d}^{(j)}$.
  if clamp_flag $== 0$ **then**
    $\xi_j = \mu \times \xi_j, j = 1, 2$.
  else
    $\xi_j = 1, j = 1, 2$.
  end if
  $T_l = T_g \times \kappa_l^{k\_\mathrm{local}}$;
  k_local $= k$_local $+ 1$.
else
  $\mathbf{y}^{(j+1)} = \mathbf{y}^{(j)}$, $\xi_j = \mu \times \xi_j$, and $j = 1, 2$.
end if
end if
end for

The given search procedure will be continued until the optimal Rx–Tx beam pair has been found. Based on the given elaborations, in the kth time (i.e., $k = k$_global $+ k$_local), the newly designed two-level annealing scheme can be summarized into

$$T(k) = T_0 \times \kappa_l^{k\_\mathrm{local}} \times \kappa_g^{k\_\mathrm{global}}, \qquad 0 < \kappa_l, \kappa_g < 1. \quad (26)$$

Notice that, during the original SA algorithm, a certain number of iterations are required at each temperature (e.g., T_l), in which the neighborhood states of $\mathbf{y}^{(i)}$ will be thoroughly exploited until the whole system has achieved the so-called "thermodynamic equilibrium" state [18], [34]. Nevertheless, in our numerical beam search problem, we have excluded this neighborhood exploitation process, as the multiple iterations may significantly increase protocol overhead and energy consumption. For the discrete and finite search space, within this newly designed two-level annealing algorithm, the local temperature decrement during the inner iteration can be considered a special kind of *neighborhood exploitation*.

C. Beam-Switching Algorithm Flows

The complete algorithm flow of the suggested beam-switching scheme, which is based on the newly designed numerical search, has been shown in Algorithms 2 and 3. As we have stated, the SA mechanics is mainly embodied by the probe moving procedure shown by the subprogram and the outer temperature update. Moreover, the decrement on outer temperature T_g is realized after the new directions have been constructed, whereas inner temperature T_l is updated after each probe moving that leads to the worse solution.

V. Experimental Simulations and Performance Evaluations

Here, we will evaluate the performance of our suggested beam-switching algorithm. For analysis convenience, the 1-D uniformly spaced antenna array is used during the following simulations and discussions. The beam codebook specified by the IEEE 802.15.3c TG is adopted in all the numerical experiments [6]. The channel condition is supposed to be quasi-static. Without loss of generality, the term in (6) coming from multipath propagation and channel noise has been normalized, i.e., $\sum_k \sum_l |\alpha_{k,\,l}|^2/\sigma_n^2 = 1$. The CM1 channel model regulated by IEEE 802.15.3c TG is used. Except for the strong line-of-sight (LOS) component with a relative gain $\Delta K = 24$ dB [29], the first-order NLOS multipath components (MPCs) are also considered. The number of NLOS clusters is $L = 5$, and the AoAs of NLOS MPCs (i.e., $\phi_{k,\,l}$) follow the zero-mean Laplacian distribution with a standard deviation of $\sigma_\phi = 20$ deg [29]. For the NLOS environment without a strong LOS component, the CM4 model is used, with $L = 5$ and $\sigma_\phi = 22.2$ deg.

A. Rosenbrock-Search-Based Beam Switching

First, we investigate the performance of the Rosenbrock-numerical-search-based beam-switching scheme. In the numerical experiment, the antenna element number N is assumed to be 32 (i.e., $N_t = N_r = N$), and we set $\chi = 2.2$, $\mu = 1.5$, $\nu = -0.7$, $\eta_1 = 0.1$, $\eta_2 = 1$, and $\eta = 1$.

Given the predefined beam codebook, the receiving SNR achieved by our beam-switching procedure, accompanying the expected SNR under the optimal beam pair $(p_{\mathrm{opt}},\ q_{\mathrm{opt}})$ using the exhaustive search, has been shown in Fig. 3(a). For thorough performance evaluation, a total of 100 independent realizations have been obtained by randomly deploying the devices' array (i.e., the normal directions), which means the best Tx–Rx beam pair $(p_{\mathrm{opt}},\ q_{\mathrm{opt}})$ has been randomly distributed in the 2-D index plane. From the simulation results, we may note that the optimal (or near-optimal) beam pair may be discovered using the Rosenbrock numerical algorithm, nevertheless, with a rough success probability of 30%. As expected, the classical numerical search is remarkably susceptible to the initial solution. A bad initialization, i.e., keeping far away from the target region containing the global solution, may easily drive the Rosenbrock search to the local maxima, leading to search failures. This is attributed to the greedy essence of the Rosenbrock method, i.e., only search movement resulting in fitness improvement is allowed [32]. Unfortunately, for this formulated beam-switching process that is shown in Fig. 2, the realistic objective function (i.e., the receiving SNR) indeed exhibits much nonsmoothness and involves numerous local optimum values, which is contradicting with the philosophy of the direct numerical search [31], [32]. To enhance the performance of the Rosenbrock search algorithm, we may further introduce SA mechanics, which allows for probabilistically accepting the worse solutions. Nevertheless, a simple combination of these two methods proved of little avail. For one thing, the exhaustive-search-based local exploitation in SA will consume considerable search steps. In addition, the search performance is still unsatisfactory. From the simulation result shown in Fig. 3(b) in which the standard geometric annealing schedule is adopted with decay constant $\kappa = 0.96$, the search failures are inevitable. A rough success ratio of this new scheme (i.e., *SA+Rosenbrock*) is about 65%, which, hence, can be hardly applied to realistic beam training process.

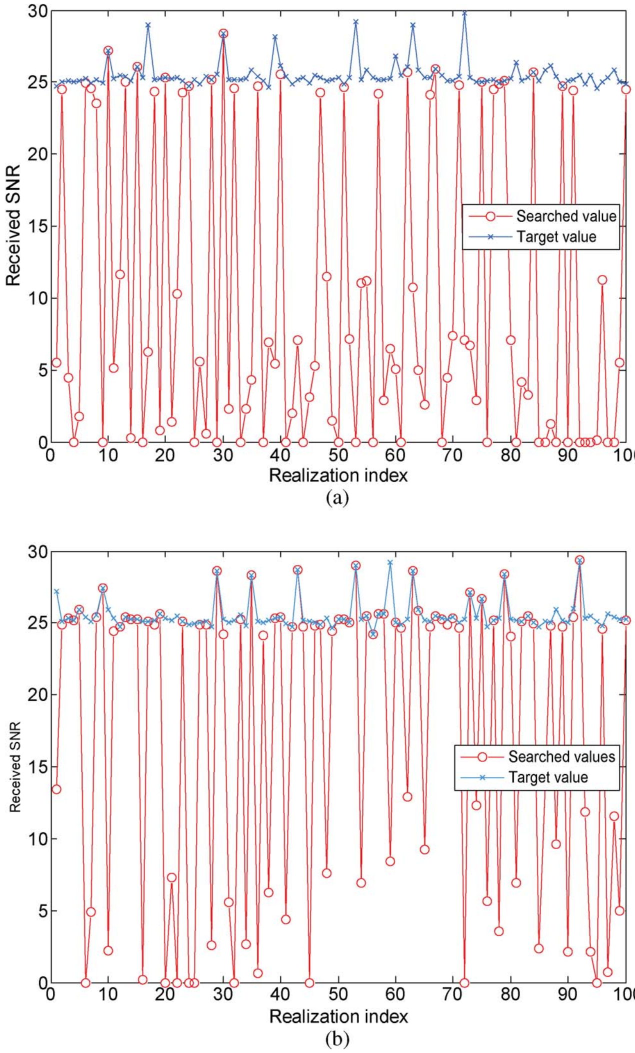

Fig. 3. Performance of the Rosenbrock numerical search in 60-GHz beam switching. (a) Rosenbrock search algorithm. (b) Rosenbrock + SA algorithm. The number of antenna elements N is 32.

B. Designed Numerical Search

We now investigate the performance of beam switching using the new numerical algorithm. Before proceeding further, we define the outage probability P_{out} of the search process. If the gap between the optimal SNR and the returned SNR has surpassed threshold ζ or the accumulated steps have exceeded a maximum number, then the outage happens. In this paper, we specify ζ to 4 dB and the maximum number to the search steps of the IEEE 802.15.3c scheme (i.e., $N_{3\mathrm{c}}$). During the simulation, the antenna element number N is set to 32. The involved parameters of the numerical search are configured as follows: $\chi = 2.2$, $\eta_1 = 0.1$, $\eta_2 = 1$, and $\eta = 1$. The initial temperature T_0 is derived from (20).

As shown in Fig. 4(a)–(d), based on the total 200 independent realizations, we have numerically derived the search complexity (i.e., the accumulated steps) and the outage probability of the new numerical-search-based beam-switching algorithm under different parameter configurations. First, we may note that, for the Rosenbrock search process, shrinkage factor ν seems to have more remarkable influences on search performance, compared with magnification factor μ, indicating that the backward operation is of critical importance to search success. To keep outage probability $P_{\mathrm{out}} = 0$ and simultaneously maintain low search complexity, the two parameters (ν and μ) should be configured carefully. Practically, we may set $\mu = 1.55$ and $\nu = -0.8$. Second, it is seen from the experimental simulations that, due to the exclusion of neighborhood exploitations in the original SA, the inner decay constant κ_l apparently has a more significant impact on search success, compared with outer decay constant κ_g. In particular, a small value of κ_l can reinforce the probability of finding the global optimum and may result in relatively higher search complexity. As a feasible compromise, we may set κ_g to 0.94 and κ_l to 0.86 in practical analysis, with a relative preference to the lower outage probability.

In Fig. 5(a) and (b), we plot the reward evolutions of the search procedure for both the Rosenbrock numerical method and the newly designed algorithm. In Fig. 5(a), a bad initialization is provided, and the Rosenbrock search fails to find the optimum and suddenly terminates, whereas the new numerical method can finally discover the best solution. It is observed that, for the greedy Rosenbrock search, the reward is gradually improved in a monotonous manner, which is finally trapped by local maxima with a termination SNR of 0.3 dB. In sharp contrast, the reward decreases can be observed in our new algorithm, except for reward improvements. By accepting worse moves, the new numerical search can wander around and obtain a more comprehensive cognition about the reward surface, and it thereby avoids being attracted by local optimum values. As the search evolves and the external temperature is further decreased, the worse movements are significantly restricted, and only prosperous probes would be allowed. Eventually, the designed search scheme can converge to the global optimum. In Fig. 5(b), we show the reward evolution with a good initialization. In this case, the Rosenbrock method could find the optimal solution. However, the required search steps of the new scheme are larger. It is emphasized that the fewer search steps of the direct numerical search become totally nonsense without the guarantee of a complete search success. After all, the blindly random initialization usually keeps far away from the unknown target in almost all cases, particularly for a larger antenna number N (e.g., $N \geq 8$).

In Fig. 5(c) and (d), we have plotted the search results of 100 independent realizations in both LOS and NLOS scenarios. First, in the presence of a strong LOS component, the new numerical algorithm can generally identify the global optimum. Due to the specified termination mechanics of the new numerical search, the output solutions are sometimes near optimal, in the sense that the outcome SNR is slightly smaller than the expected SNR by 0–2 dB. Second, in the NLOS environment, where several NLOS MPCs may become comparable relatively, the designed algorithm may still find the optimal or suboptimal solutions, only with more optimal solutions replaced by suboptimum values. Notice that, for the SNR surface without a dominant ascending region, the effort to identify the global optimum may become impractical and invaluable, given the considerably increased search complexity. The required search steps are plotted in Fig. 5(d). It is evaluated from an averaging

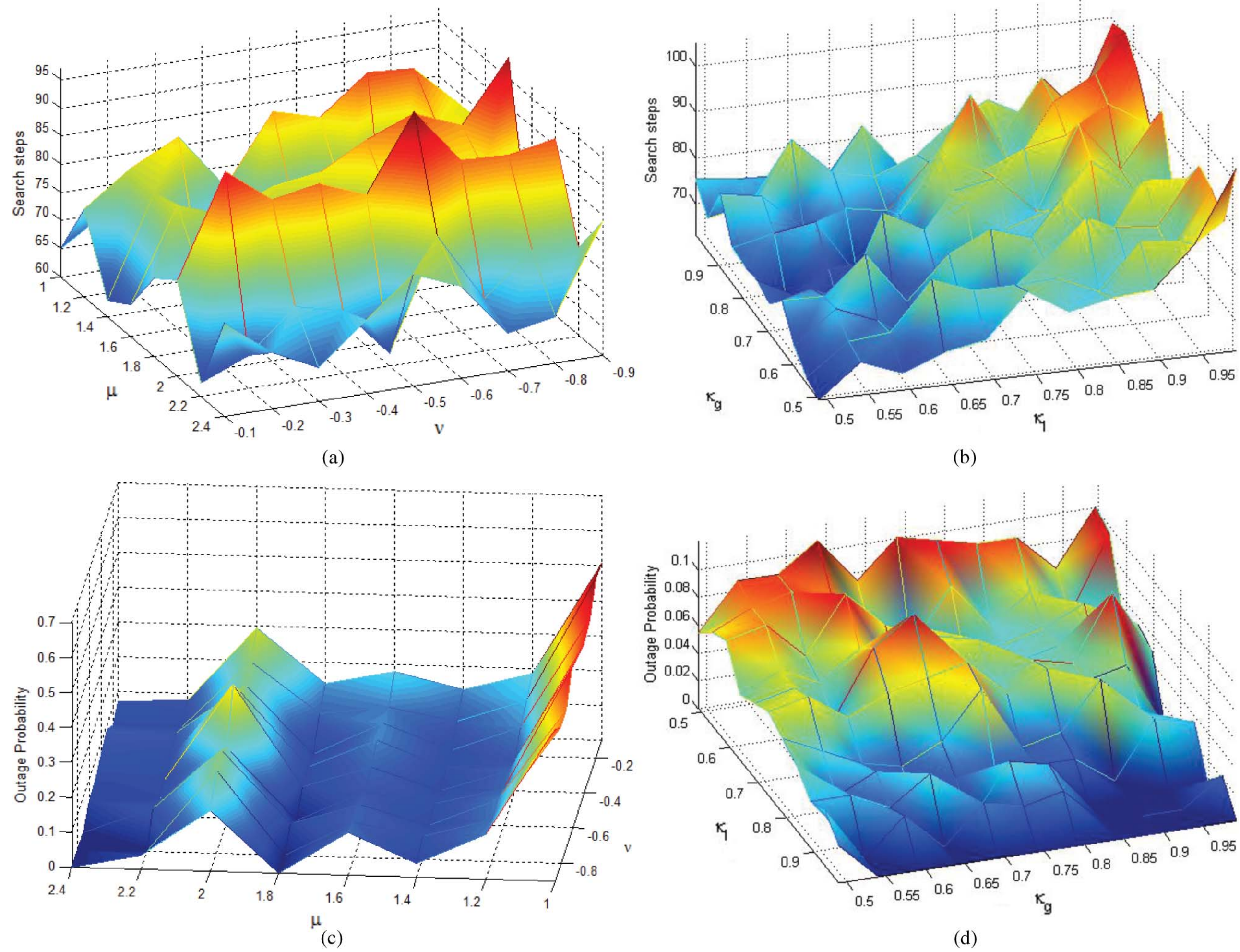

Fig. 4. Effects on the beam-switching performance from the decrement constants in the designed numerical search. (a) Search complexity (i.e., the accumulated search steps) under different μ and ν. (b) Search complexity (i.e., the accumulated search steps) under different κ_l and κ_g. (c) Outage probability under different μ and ν. (d) Outage probability under different κ_l and κ_g. Notice that the results are derived from total 200 independent realizations.

of 100 independent realizations that the expected search steps are about 74 in the LOS case, whereas for the NLOS scenario, these expected search steps are about 37.

C. Beam-Switching Performance Evaluation

In this experiment, we will give the comprehensive performance evaluation of our proposed beam-switching scheme. We first investigate the search complexity of the two-stage scheme in IEEE 802.15.3c. Without loss of generality, in our experiment, the Tx and Rx antenna elements are both set to N, with the prescribed sector number of $N^{(1)}$. Compared with the complete exhaustive search, from (7), the search complexity reduction is essentially attributed to the sector-level presearch introducing an *asymptotic* factor $(1/N^{(1)})^2$. For different values of $N^{(1)}$, the search complexity is shown in Fig. 6. Notice that, due to realization considerations, sector number $N^{(1)}$ cannot be arbitrarily large in practice, and the maximum sector number is assumed to be 4. As expected, there indeed exists an optimal sector number for different antenna elements, which may complicate protocol flow to some extent to minimize the search steps. Meanwhile, the accumulated steps still follow the complexity tendency of $O(N^2)$. With the further increase in the number of elements, the search complexity may become uncontrollable, accompanying protocol overhead and energy consumption.

In Fig. 6, we also give the average complexity of the suggested scheme using the new numerical search. Although with much lower probability of occurrence (e.g., $< 3\%$), the maximum steps have been plotted together. First, notice that, as the antenna elements increase, the search complexity is gently increased in both the LOS and NLOS scenarios, which is in contrast to the sharp growing of the IEEE.802.15.3c scheme. That is, the curse of search dimension can be alleviated by the presented algorithm. In particular, for the new scheme, the required steps are about 74 in the LOS environment and 37 in the NLOS case when N is 32. In comparison, the two-stage search scheme needs 128 preamble transmissions. When $N = 64$, the two-stage search may even need 320 transmissions. This search complexity may greatly burden overhead and consume considerable power, which makes the current start-of-the-art beam-switching techniques impractical for 60-GHz WPANs. Nevertheless, the required search steps of our proposed algorithm, in the case of 64 elements, are only 147 in LOS environments, which may shows remarkable advantage over the other existing methods.

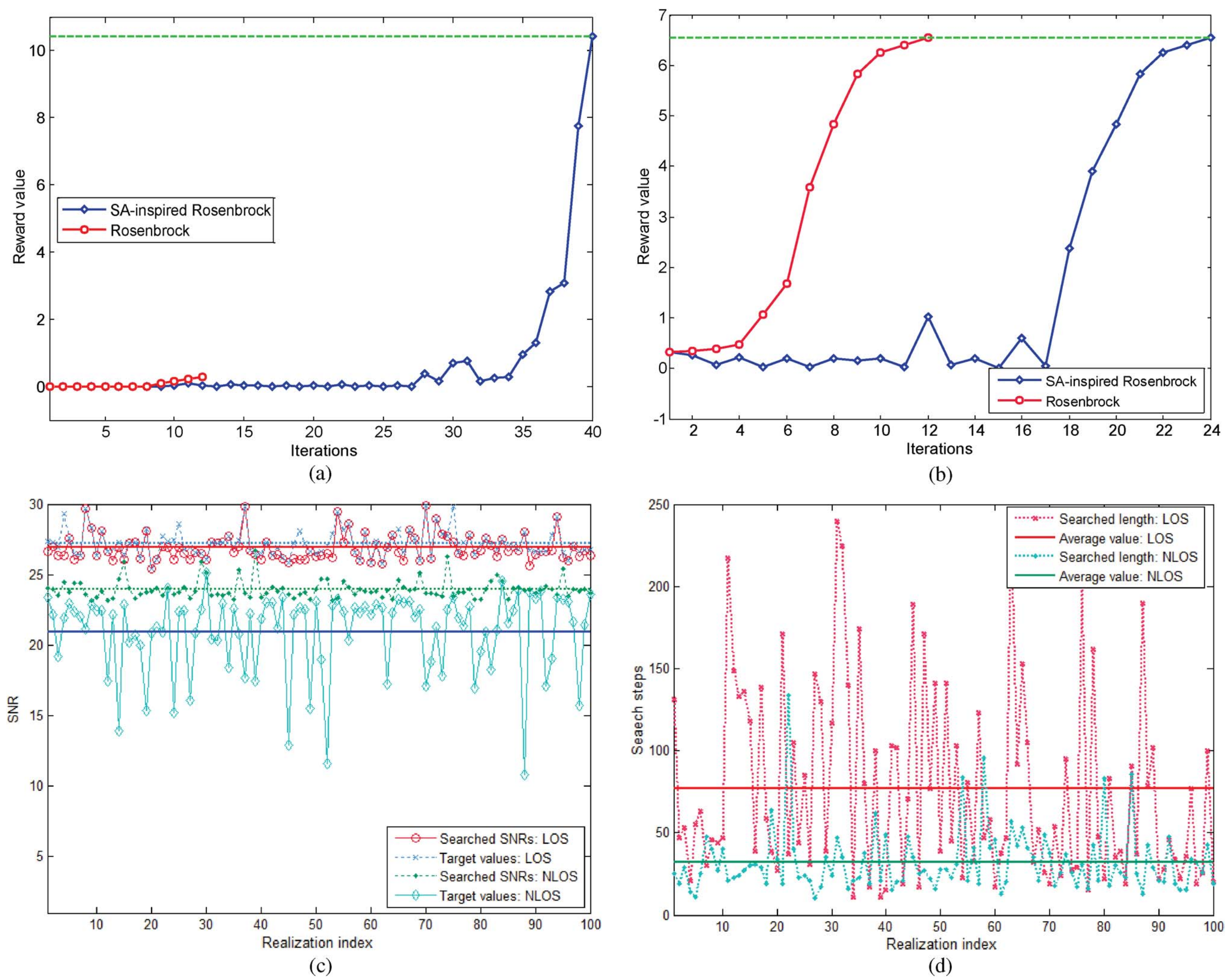

Fig. 5. Search performance of the Rosenbrock algorithm and the new numerical algorithm. (a) With a bad initialization near the local optimum. (b) With a fair initialization near the global optimal solution. Notice that the global optimal reward is also plotted by the dotted line. (c) Achieved reward using the new search algorithm. (d) Accumulated search steps of 100 independent algorithm realizations. The number of antenna elements N is set to 32.

The average values of searched SNRs are plotted in Fig. 7 under different antenna elements. In our analysis, the searched SNRs represent the received SNRs returned by the proposed beam-switching algorithm, whereas the target SNRs are evaluated statistically based on 100 independent experiments. That is, during each experimental simulation, we assume that the optimal beam pair is uniquely distributed in the 2-D search plane. Then, the unknown optimal SNR is obtained by an exhaustive search. As the number of antenna elements increases, in the presence of LOS MPCs, we may note that the searched SNRs will remarkably improve with the increased elements. Simultaneously, the SNR gap between the searched SNRs and the optimal SNRs has also been widened. In other words, with the significantly growing search space, it is supposed that the optimum values may be replaced by the suboptimal solutions. For the NLOS case with the SNR surface involving many comparable peaks, it is seen from the experimental results that the searched SNRs may not be improved significantly when $N > 32$. It seems that, in this case, the achieved SNRs may even become converged. While the number of antenna elements is relatively small (e.g., $N \leq 32$), it is considered that the proposed numerical search-based beam-switching scheme can be still applied in NLOS environments.

Now, we may simply evaluate the energy efficiency of the given two BF training methods. We denote the emission power by P_e in each training round. In the two-stage scheme, the total search rounds are K_1, and the consumed power may be measured by $\Omega_1 = K_1 \times P_e$. For the suggested beam-switching scheme, the calculation process also consumes P_c, except for the emission power P_e. If the search rounds are K_2, then the required power is given by $\Omega_2 = K_2 \times (P_e + P_c)$. Notice that we usually have $P_e \gg P_c$ in practice. Thus, the energy consumption is basically proportional to the search complexity (i.e., K_1 or K_2). In Fig. 6, we may conclude that the energy efficiency of the suggested BF training can be significantly improved.

D. Other Considerations

Except for the great advantage in search performance by significantly reducing protocol overhead accompanying energy consumption, our method also simplifies the protocol design in 60-GHz BF training. For the IEEE 802.15.3c scheme, three

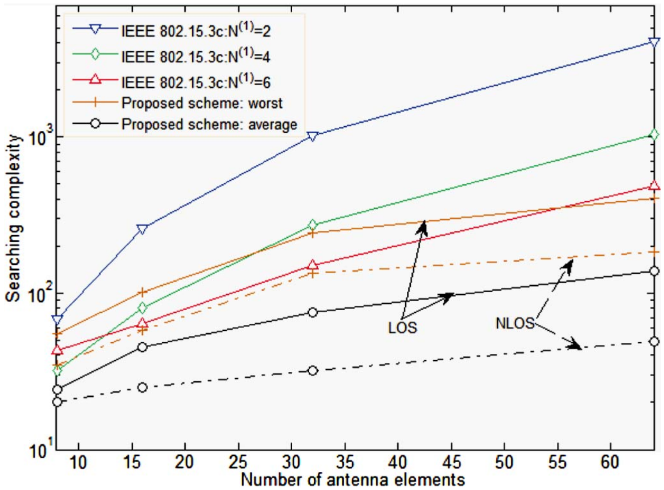

Fig. 6. Performance evaluation of the presented beam-switching scheme. The accumulated search steps of the proposed algorithm are numerically derived by an averaging on 200 realizations.

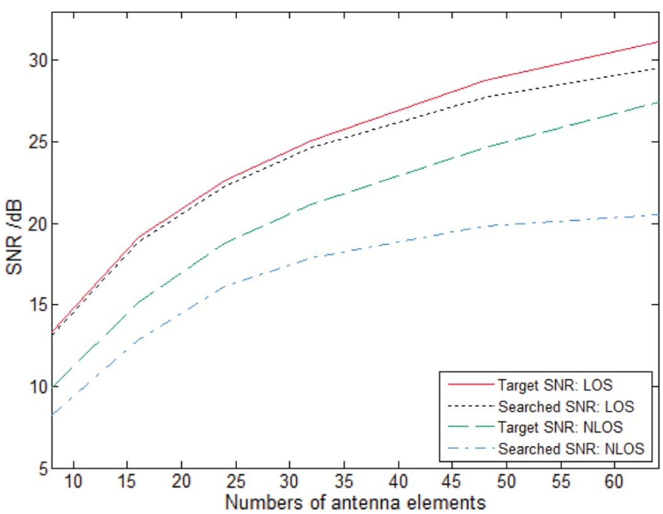

Fig. 7. Average searched SNRs under different numbers of antenna elements.

antenna patterns should be supported [4], and with sector beam patterns, the initial link establishment may fail due to the limited array gain. A similar difficulty may occur to the presearch process in [33]. Meanwhile, the optimal sector number (i.e., $N^{(1)}$) should be determined according to different antenna configurations to minimize search steps. For the Tx and Rx antennas with different elements, i.e., $N_t \neq N_r$, the given situations will become more prominent. Nevertheless, during the designed numerical scheme, the beam-training process is independent of antenna configuration and protocol, which is of great significance to practical applications.

VI. Conclusion

We present a new BF training algorithm for 60-GHz millimeter-wave communications. The beam-switching procedure is formulated as an appealing optimization problem that can be solved by a numerical search. To overcome the defects of traditional greedy numerical schemes, a more promising numerical optimization algorithm inspired by SA mechanics is further suggested. By designing a novel two-level temperature adjustment scheme, the developed numerical search may basically escape from the local optimum, which is, hence, much superior to classical direct numerical methods and thereby of great promise to realistic optimization. Finally, with the protocol overhead and energy consumption significantly reduced, the formulated beam switching is efficiently realized by the new numerical algorithm. Experimental simulations further validate our suggested beam-switching algorithm. Even for a large number of antenna elements, in which the other popular schemes become impractical due to the unaffordable time and energy consumption, the suggested algorithm may still operate well. In future research, theoretical analysis on algorithm convergence will be investigated, which is important to more general applications.

Acknowledgment

The authors would like to thank three anonymous reviewers for their thoughtful and constructive remarks that are helpful in improving the quality of this paper.

References

[1] S. Lakshmanan, K. Sundaresan, R. Kokku, A. Khojestepour, and S. Rangarajan, "Towards adaptive beamforming in indoor wireless networks: An experimental approach," in *Proc IEEE INFOCOM*, 2009, pp. 2621–2625.
[2] T. Baykas, C. S. Sum, Z. Lan, J. Y. Wang, M. A. Rahman, and H. Harada, "IEEE 802.15.3c: The first IEEE wireless standard for data rates over 1 Gb/s," *IEEE Commun. Mag.*, vol. 49, no. 7, pp. 114–121, Jul. 2011.
[3] N. Guo, R. C. Qiu, S. S. Mo, and K. Takahashi, "60-GHz millimeter-wave radio: Principle technology, and new results," *EURASIP J. Wireless Commun.*, vol. 2007, pp. 68253-1–68253-8, Dec. 2006.
[4] P. Smulders, "Exploiting the 60 GHz band for local wireless multimedia access: Prospects and future directions," *IEEE Commun. Mag.*, vol. 40, no. 1, pp. 140–147, Jan. 2002.
[5] J. Wang, Z. Lan, C. Pyo, C. Sum, T. Baykas, J. Gao, A. Rahman, R. Funada, F. Kojima, H. Harada, and S. Kato, "Beam-forming codebook design and performance evaluation for millimeter-wave WPAN," in *Proc. IEEE VTC*, Anchorage, AK, USA, Sep. 20-23, 2009, pp. 1–6.
[6] *Part 15.3: Wireless Medium Access Control (MAC) and Physical Layer (PHY) Specifications for High Rate Wireless Personal Area Networks (WPANs)*, IEEE Std. 802.15.3c, 2009. [Online]. Available: http://www.ieee802.org/15/pub/TG3.html
[7] *Part 11: Wireless LAN Medium Access Control (MAC) and Physical Layer (PHY) Specifications -Amendment 6: Enhancements for Very High Throughput in the 60 GHz Band*, IEEE P802.11ad draft amendment D0.1, 2010.
[8] R. Fletcher and C. M. Reeves, "Function minimization by conjugate gradients," *Comput. J.*, vol. 7, no. 2, pp. 149–154, 1964.
[9] H. H. Rosenbrock, "An automatic method for finding the greatest or least value of a function," *Comput. J.*, vol. 3, no. 3, pp. 175–184, 1960.
[10] H. H. Rosenbrock, "Some general implicit processes for the numerical solution of deferential-equations," *Comput. J.*, vol. 5, no. 4, pp. 329–330, 1963.
[11] H. H. Rosenbrock, *An Automatic Method for Unconstrained Optimization Problems*. New York, NY, USA: American Elsevier, 1968.
[12] P. M. Pardalos and G. C. Mauricio Resende, *Handbook of Applied Optimization*. Oxford, U.K.: Oxford Univ. Press, 2001.
[13] J. A. Nelder and R. Mead, "A simplex method for function minimization," *Comput. J.*, vol. 7, no. 4, pp. 308–313, 1965.
[14] M. J. D. Powell, "An efficient method of finding the minimum of a function of several variables without calculating derivatives," *Comput. J.*, vol. 7, no. 2, pp. 155–162, 1964.
[15] J. Bang-Jensen, G. Gutin, and A. Yeo, "When the greedy algorithm fails," *Discrete Optim.*, vol. 1, no. 2, pp. 121–127, Nov. 2004.
[16] S. Kirkpatrick, C. D. Gelatt, and M. P. Vecchi, "Optimization by simulated annealing," *Science*, vol. 220, no. 4598, pp. 671–680, May 1983.

[17] K. Binder and D. Stauffer, *A Simple Introduction to Monte Carlo Simulations and Some Specialized Topics, in Applications of The Monte Carlo Method in Statistical Physics*, K. Binder, Ed. Berlin, Germany: Springer-Verlag, 1985, pp. 1–36.

[18] P. J. M. van Laarhoven and E. H. L. Aarts, *Simulated Annealing: Theory and Applications*. Dordrecht, The Netherlands: Reidel, 1987.

[19] E. Arts and J. Korst, *Simulated Annealing and Boltzmann Machines: A Stochastic Approach to Combinatorial Optimization and Neural Computing*. New York, NY, USA: Wiley, 1989.

[20] E. H. L. Aarts and P. J. M. Laarhoven, "Statistical cooling: A general approach to combinatorial optimization problems," *Philips J. Res.*, vol. 40, no. 4, pp. 193–226, 1985.

[21] L. Ingber, "Adaptive simulated annealing (ASA): Lessons learned," *Control Cybern.*, vol. 25, no. 1, pp. 33–54, 1996.

[22] Amendment of parts 2, 15 and 97 of the commission's rules to permit use of radio frequencies above 40 GHz for new radio applications, Fed. Commun. Comm., Washington, DC, USA, 1995. [Online]. Available: ftp://ftp.fcc.gov/pub/Bureaus/Engineering_Technology/Orders/1995/fcc95499.txt

[23] H. Ikeda and Y. Shoji, 60 GHz Japanese regulations, IEEE Std. 802.15-05-0525-03, Oct. 2006.

[24] Frequency Range 29.7 MHz to 105 GHz and Associated European Table of Frequency Allocations and Utilizations, Eur. Radio Commun. Comm., Copenhagen, Denmark, 1995. [Online]. Available: http://www.ero.dk

[25] C. R. Anderson and T. S. Rappaport, "In-building wideband partition loss measurements at 2.5 and 60 GHz," *IEEE Trans. Wireless Commun.*, vol. 3, no. 3, pp. 922–928, May 2004.

[26] N. Celik, M. F. Iskander, R. Emrick, S. J. Franson, and J. Holmes, "Implementation and experimental verification of a smart antenna system operating at 60 GHz band," *IEEE Trans. Antennas Propag.*, vol. 56, no. 9, pp. 2790–2880, Sep. 2008.

[27] J. H. Winters, "Smart antennas for wireless systems," *IEEE Personal Commun.*, vol. 5, no. 1, pp. 23–27, Feb. 1998.

[28] J. R. Foerster, M. Pendergrass, and A. F. Molisch, "Channel model for ultra-wideband personal area networks," *IEEE Wireless Commun.*, vol. 10, no. 6, pp. 14–21, Dec. 2003.

[29] K. Sato, H. Sawada, and Y. Shoji, "Channel model for millimeter wave WPAN," in *Proc. IEEE 18th Int. Symp. PIMRC*, Athens, Greece, Sep. 2007, pp. 1–5.

[30] S. Yoon, T. Jeon, and W. Lee, "Hybrid beam-forming and beam-switching for OFDM based wireless personal area networks," *IEEE J. Select. Areas Commun.*, vol. 27, no. 8, pp. 1425–1432, Oct. 2009.

[31] R. Hooke and T. A. Jeeves, "Direct search solution of numerical and statistical problems," *J. Ass. Comput. Mach.*, vol. 8, no. 2, pp. 212–229, Apr. 1961.

[32] V. J. Orczon, "On the convergence of pattern search algorithm," *SIAM J. Optim.*, vol. 7, no. 1, pp. 1–25, Feb. 1997.

[33] B. Li, Z. Zhou, W. X. Zou, and G. L. Du, "On the efficient beam-forming training for 60GHz wireless personal area networks," *IEEE Trans. Wireless Commun.*, vol. 12, no. 2, pp. 504–515, Feb. 2013.

[34] C. J. Chang and C. H. Wu, "Optimal frame pattern design for a TDMA mobile communication system using a simulated annealing algorithm," *IEEE Trans. Veh. Technol.*, vol. 42, no. 2, pp. 205–211, May 1993.

[35] D. H. Johnson and D. E. Dudgeon, *Array Signal Processing*. Englewood Cliffs, NJ, USA: Prentice Hall, 1993.

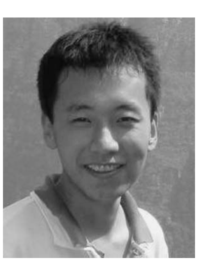

Bin Li received the Bachelor's degree in electrical information engineering from Beijing University of Chemical Technology, Beijing, China, in 2007 and the Master's degree in communication and information engineering from Beijing University of Posts and Telecommunications (BUPT) in 2009. He is currently working toward the Ph.D. degree in communication and information systems with BUPT.

His current research interests include bio-inspired intelligent optimization algorithms, channel modeling, signal processing algorithms for ultrawideband, wireless sensor networks, millimeter-wave communications, and cognitive radios. He is the author of more than 40 journal and conference papers.

Dr. Li has served as a regular Reviewer for the IEEE SIGNAL PROCESSING LETTERS, the IEEE TRANSACTIONS ON COMMUNICATIONS, and the IEEE TRANSACTIONS ON SIGNAL PROCESSING. He received the Excellent Ph.D. Student Award from BUPT in 2010 and 2011 and the Best Paper Award at the Sixth International Conference on Communications and Networking in China in 2011.

Zheng Zhou (M'05) received the Bachelor's degree from Harbin Institute of Military Engineering, Harbin, China, in 1967 and the Master's and Ph.D. degrees from Beijing University of Posts and Telecommunications, Beijing, China, in 1982 and 1988, respectively, all in electrical engineering.

From 1993 to 1995, he was a Visiting Research Fellow with the Department of Information Engineering, Chinese University of Hong Kong, Hong Kong, through the support of Hong Kong Telecom International Postdoctoral Fellowship. In 2000, he was an Invited Overseas Researcher with Japan Kyocera DDI Future Communication Research Institute (supported by the Japan Key Technology Center). From 1998 to 2003, he was the Vice Dean of the School of Telecommunication Engineering, BUPT, where he is currently a Professor.

Dr. Zhou was a member of the Technical Subcommittee on Cognitive Networks of the IEEE Communications Society and the International Steering Committee of the IEEE International Symposium on Communications and Information Technologies (IEEE ISCIT) from 2003 to 2010 and the Co-chair of the Technical Program Committee of the IEEE ISCIT in 2005. He was also the General Vice Chair of the First IEEE International Conference on Communications and Networking in China (IEEE ChinaCom) in 2006 and a Steering Committee Member of the Second IEEE ChinaCom in 2007. He is a voting member and a contributor of the IEEE 802.15 Task Group (TG3a and TG4a), a Senior Member of China Institution of Communications (CIC), a member of the Radio Application and Management Technical Committee of CIC, a Senior Member of China Computer Federation (CCF), a member of the Sensor Network Technical Committee of CCF, an H subcommittee member of the China Radio Interference Standard Technology Committee, the General Secretary of the China Ultrawideband Forum, and the General Secretary of the China Bluetooth Forum.

Haijun Zhang is currently working toward the Ph.D. degree with the School of Information and Communication Engineering, Beijing University of Posts and Telecommunications (BUPT), Beijing, China.

From September 2011 to September 2012, he was a Visiting Researcher with the Center for Telecommunications Research, King's College London, London, U.K., through the support of the China Scholarship Council. His current research interests include game theory, radio resource allocation and management, interference management in heterogeneous networks, green radios, and physical-layer security.

Arumugam Nallanathan (S'97–M'00–SM'05) received the B.Sc. degree with honors from the University of Peradeniya, Sri-Lanka, in 1991, the CPGS degree from the University of Cambridge, Cambridge, U.K. in 1994, and the Ph.D. degree from the University of Hong Kong, Hong Kong, in 2000, all in electrical engineering.

From August 2000 to December 2007, he was an Assistant Professor with the Department of Electrical and Computer Engineering, National University of Singapore, Singapore. From 2011 to 2012, he was the Head of Graduate Studies with the School of Natural and Mathematical Sciences, King's College London, London, U.K. He is currently a Professor of wireless communications with the Institute of Telecommunications, King's College London, London, U.K. He is the author of more than 200 journal and conference papers. His research interests include smart grid, cognitive radio, and relay networks.

Mr. Nallanathan currently serves as the Chair for the Signal Processing and Communication Electronics Technical Committee of the IEEE Communications Society. He served as the General Track Chair for the IEEE Vehicular Technology Conference and the Co-chair for the Symposium on Signal Processing for Communications of the IEEE Global Telecommunications Conference (IEEE GLOBECOM) in 2008, the Co-Chair for the Wireless Communications Symposium of the IEEE International Conference on Communications (IEEE ICC) in 2009, the Co-Chair for the Signal Processing for Communications Symposium of the IEEE GLOBECOM and the Co-Chair for the Technical Program Committee of the IEEE International Conference on Ultrawideband in 2011, the Co-Chair for the Signal Processing for Communications Symposium of the IEEE ICC in 2012, and the Co-Chair for the Communications Theory Symposium of the IEEE GLOBECOM in 2013. He serves as the Technical Program Co-Chair (Medium Access Control Track) for the IEEE Wireless Communications and Networking Conference in 2014. He was an Editor for the IEEE TRANSACTIONS ON WIRELESS COMMUNICATIONS, IEEE WIRELESS COMMUNICATIONS LETTERS, and IEEE SIGNAL PROCESSING LETTERS, and a Guest Editor for the *European Association for Signal Processing Journal on Wireless Communications and Networks: Special Issue on UWB Communication Systems—Technology and Applications*. He is an Editor for IEEE the TRANSACTIONS ON COMMUNICATIONS and the IEEE TRANSACTIONS ON VEHICULAR TECHNOLOGY. He coreceived the Best Paper Award at the 2007 IEEE International Conference on Ultrawideband. He received the IEEE Communications Society Signal Processing and Communications Electronics Outstanding Service Award in 2012.